

E. WELCOMME<sup>1</sup>  
P. WALTER<sup>1,✉</sup>  
P. BLEUET<sup>2</sup>  
J.-L. HODEAU<sup>3</sup>  
E. DOORYHEE<sup>3</sup>  
P. MARTINETTO<sup>3</sup>  
M. MENU<sup>1</sup>

# Classification of lead white pigments using synchrotron radiation micro X-ray diffraction

<sup>1</sup> Centre de Recherche et de Restauration des Musées de France – CNRS UMR 171,  
14, quai François Mitterrand, 75001 Paris, France

<sup>2</sup> European Synchrotron Radiation Facility, BP 220, 38043 Grenoble Cedex, France

<sup>3</sup> Institut Néel, CNRS-UPR 503-1, 25, Av. des Martyrs, BP 166, 38042 Grenoble Cedex 9, France

Received: 12 January 2007 / Accepted: 25 June 2007

Published online: 24 August 2007 • © Springer-Verlag 2007

**ABSTRACT** Lead white pigment was used and synthesised for cosmetic and artistic purposes since the antiquity. Ancient texts describe the various recipes, and preparation processes as well as locations of production. In this study, we describe the results achieved on several paint samples taken from Matthias Grünewald's works. Grünewald, who was active between 1503 and 1524, was a major painter at the beginning of the German Renaissance. Thanks to X-ray diffraction analysis using synchrotron radiation, it is possible to associate the composition of the paint samples with the masters ancient recipes. Different approaches were used, in reflection and transmission modes, directly on minute samples or on paint cross-sections embedded in resin. Characterisation of lead white pigments reveals variations in terms of composition, graininess and proportion of mineral phases. The present work enlightens the presence of lead white as differentiable main composition groups, which could be specific of a period, a know-how or a geographical origin. In this way, we aim at understanding the choices and the trading of pigments used to realise paintings during northern European Renaissance.

PACS 61.10.Nz; 07.85.Qe; 61.43.Gt

## 1 Introduction

Used extensively since antiquity for cosmetic [1] and painting purposes, lead white is one of the eldest man-made pigments, and its history dates back to ancient Greece. Theophrastus, Pliny and Vitruvius all described its preparation from metallic lead and vinegar and how it was used [2, 3]. Other chemical processes used to elaborate this pigment have been developed from the Renaissance period to the end of the XIXth century. During the Renaissance period, lead white was extensively used in European easel paintings [4]. This dense pigment was chosen owing to its optical properties and its known catalytic effect in speeding up the drying due to the action of lead upon oil [5]. However, it was partly replaced in the 19th century, for toxicity reasons, by zinc white and almost fully replaced in the 20th century by titanium white.

Its mineral composition is generally considered to be hydrocerussite ( $2\text{PbCO}_3 \cdot \text{Pb}(\text{OH})_2$ ) but classical examinations by optical microscopy and electron scanning microscopy routinely carried out on pigments to identify their elemental composition, do not allow an accurate mineralogical identification. However, X-ray diffraction analysis of some samples has shown that a cerussite phase is detected too. This analytical mean allows discriminating between the two phases of lead carbonates and provides quantitative mineralogical information. In this case, laboratory X-ray diffraction is not appropriate for the analysis of small quantities of material or when mixtures of compounds are present through a complex paint stratigraphy. Due to the difficulty in identifying and quantifying these pigments with conventional techniques, synchrotron radiation was used in the search for higher angle and spatial resolutions at the European synchrotron radiation facility (ESRF), at the beamlines ID31 and ID22.

We will demonstrate, thanks to our analysis on several painting samples from the beginning of the Renaissance that lead white can be a mixture of hydrocerussite and cerussite, or only cerussite ( $\text{PbCO}_3$ ). The objective of our work is to study the variation in the pigment composition, which could be linked to different geographical origins or manufacturing processes. Through crystallographic analysis with synchrotron light, we shall establish a classification of the pigments to gain a better understanding of the historical documents (inventory of artist's workshop, list of products known, etc.) and of the recipes described by ancient authors [6]. We aim at understanding why various lead white pigments have been used by northern European painters at the beginning of the Renaissance. Three different X-ray diffraction-based strategies for analysing fragments of historical paint are compared and discussed.

## 2 Experimental

### 2.1 Analytical techniques

A first approach consists of characterising cross-sections of paint samples as usually prepared for microscopic observation or scanning electron microscope analysis. The composition of the bulk sample embedded in resin was determined by high-resolution diffraction at the beamline ID31 at the ESRF. The incident beam size is  $5 \text{ mm} \times 1 \text{ mm}$  ( $H \times V$ ). A bank of nine scintillation detectors (Ge crystals) is scanned

✉ Fax: +33(0)147033246, E-mail: philippe.walter@culture.gouv.fr

vertically to measure the diffracted intensity as a function of  $2\theta$  angle [7]. High energy X-rays (28.8 keV) were chosen to work in the Debye–Scherrer transmission mode. To limit the diffusion of X-rays by the resin, the resin was thinned down to 1 mm. The acquisition time was 4 h. Fullprof software [8] was used to perform a Rietveld refinement analysis from the high-resolution diffraction patterns in order to determine the relative phase abundance of multiphase sample [9]. It appears as a convenient alternative method when the use of traditional approaches is difficult due to severe line overlapping [10]. The presence of several pigment mixtures and especially lead carbonates mixtures, of which the lines overlap significantly on the whole diffraction diagram, requires the application of this refinement method.

A second approach (Fig. 1a) consists of using micro-X-ray diffraction ( $\mu$ -XRD) in reflection mode on painting cross sections embedded in resin. A beam size of about  $3.8 \times 1.4 \mu\text{m}$  ( $H \times V$ ) allows identification and quantification of the proportions of the different mineral phases in a selected layer. The experiments were achieved at the ID22

beamline [11] which provides a panel of complementary microanalyses and microimaging techniques ( $\mu$ -XRD, micro-X-ray fluorescence ( $\mu$ -XRF), micro-X-ray Absorption Near Edge Structure ( $\mu$ XANES), and absorption-contrast tomography). This supplies important information about the nature of the pigments. The X-ray energy was fixed at 16 keV. The flux was estimated to be  $1.2 \times 10^{10}$  photons/s. A photonics science CCD camera was used for collecting X-ray diffraction patterns (acquisition time from 1 to 30 s). The X-ray fluorescence spectra were simultaneously detected with a Si(Li) detector (Gresham) [12]. The correlation between fluorescence and diffraction data helps in completing the data interpretation.

Three line scans of analysis were realised in each painting cross-section. During measurement, we obtained a two-dimensional signal on the camera. After corrections, the Debye-Scherrer diffraction rings are unwrapped and integrated vs. the azimuthal angle to produce the normal 1D diffraction pattern thanks to the ESRF package Fit2D [13]. So, each diffraction pattern corresponds to one pixel on the line

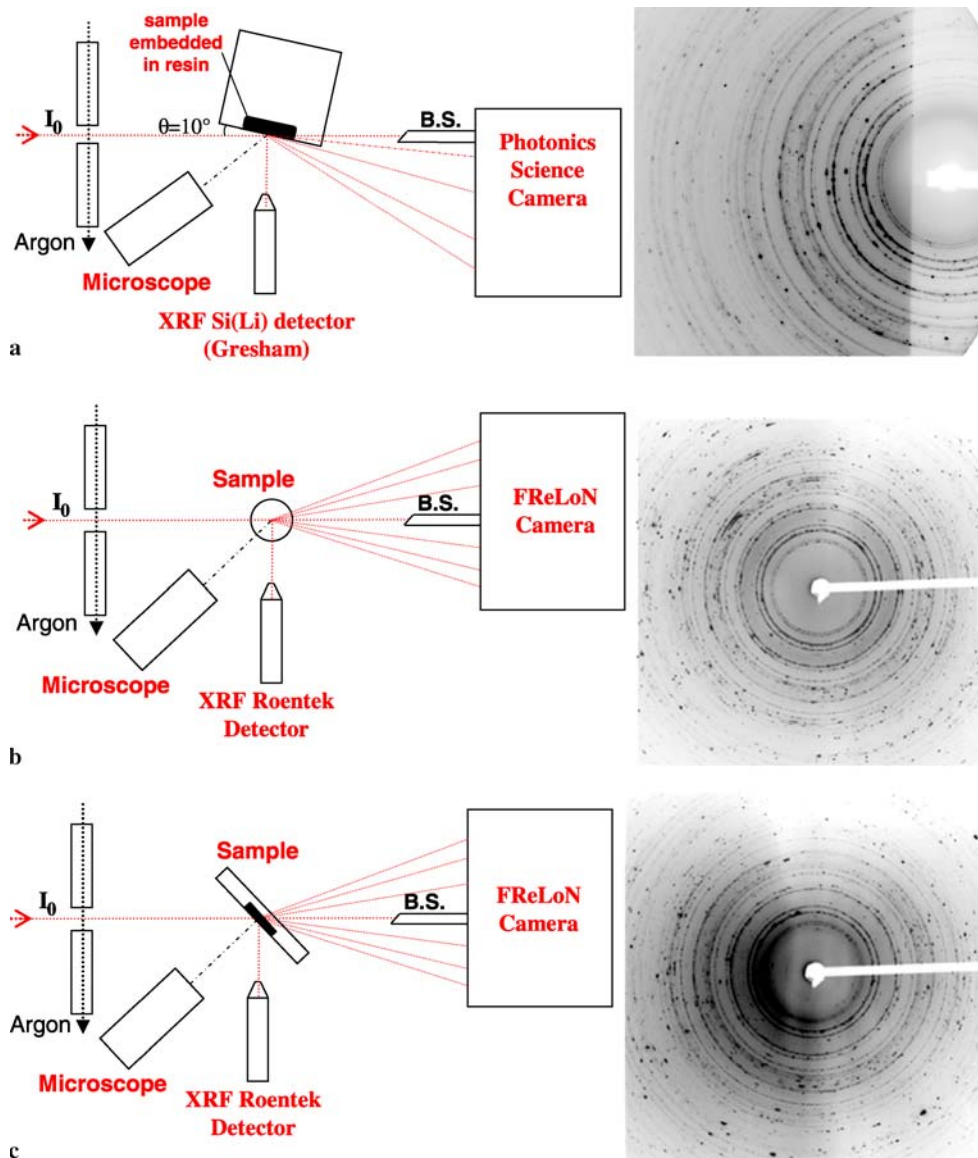


**FIGURE 1** Experimental setups for paint analysis at the ID22-ESRF beamline and 2D images of the diffraction rings obtained in each case. (a) Analysis by SR- $\mu$ XRD in reflection mode on painting cross-section embedded in resin. The angle of the incident beam against the sample is estimated to be  $10^\circ$ . (b) Analysis by SR- $\mu$ XRD in transmission mode directly on the sample. (c) Analysis by SR- $\mu$ XRD in transmission mode on a thin painting cross-section to maintain a correct orientation of the different layers. B.S.: beamstop

of analysis through the different layers of pigments. Then we performed the quantitative analysis by applying the Rietveld method.

A similar approach was used by Salvado et al. [14] with a larger beam footprint (100  $\mu\text{m}$ ) on a gothic Spanish painting. In our case, application of  $\mu\text{-XRD}$  can help to exhibit non-uniformities such as, a large variation in the phase composition or in the grain size. For instance, intense spots are observed on the diffraction image when the powder is made of coarse grains whereas continuous lines are characteristic of a fine powder at the scale of the beamsize.

A third approach (Fig. 1b and c) consists of using  $\mu\text{-XRD}$  in transmission mode directly on the sample without any sample preparation. This technique avoids the resin contribution to the diffraction signal. The painting samples were stuck on 400  $\mu\text{m}$  diameter capillaries. We have also analysed thin cross sections in resin to have a better control of the orientation of the pigment layers: the plane of the cross-section is perpendicular to the axis of the beam. The X-ray energy was fixed at 18 keV and the beam size was  $2.9 \times 1.5 \mu\text{m}^2$ . A FReLoN 2000 CCD camera [15] was used for collecting the X-ray diffraction patterns (acquisition time = 1 s) simultaneously with XRF spectra. A scan of  $40 \times 50$  pixels corresponding to an area of  $100 \times 120 \mu\text{m}^2$  was obtained after 4 h. The flux was approximately  $9.8 \times 10^{10}$  photons/s.

For  $\mu\text{-XRD}$  analysis, the set-up included a focusing stage, a pinhole stage, a XYZ sample scanning stage, a video microscope, a fluorescence, diffraction and normalization detectors.

## 2.2 Samples

The analysis was performed on painting cross-sections from two artworks of Matthias Grünewald: the Isenheim altarpiece painted between 1512 and 1515–1516, kept at the Unterlinden Museum at Colmar and the Crucifixion painted at around 1500–1508 and kept in the Kunstmuseum, Basel. The analytical work on these masterpieces takes part in a global research work on the painting technique of Matthias Grünewald who was one of the major painters of the German Renaissance during the first part of the XVIth century. The first and main results of this general research were presented at the international conference at Colmar focused on “the pictorial technique of Grünewald and his peers” (January 2006), to be published in *Eu-Artech*, éd. C2RMF.

The Isenheim altarpiece is a complex structure, with two sets of folding wings. It is composed of nine large panels which are 3 m high and 1.65 m large. The panels are gathered on three sets of wings and one predella. The central panel in

the closed position offers one of the most striking illustrations of the Crucifixion ever represented in art. The Lamentation (or the settings with the tomb) is the subject of the predella. On the two lateral wings are depicted Saint Anthony and Saint Sebastian. When the outer wings are opened, three scenes of celebration are revealed: from left to right the Annunciation, the Concert of angels, the Nativity and the Resurrection. The second opening allows one to discover on both sides two panels which represent the Visit of Saint Anthony to Saint Paul the Hermit and the Temptation of Saint Anthony. These panels surround a carved wood reliquary, made by Nicolas of Haguenau in 1505.

In this altarpiece, the use of many superimposed paint layers shows that Grünewald had a thorough knowledge of the pictorial matter that allowed him to play with the light and the colours [16]. It is a correct support to the present study since the long period of time needed for the altarpiece’s execution (four years) could permit to observe possible variation in the pigment composition. Moreover, after Grünewald’s death, an inventory of his property was drawn up where colours and tools that he used were mentioned [6].

The sampling was carried out from highlights where small damages already exist, or on edges of the panels with the help of a microscalpel. For this study we were interested in seven painting samples and their cross sections (the list is described in Table 1). The samples are very small in size (100  $\mu\text{m} \times 400 \mu\text{m} \times 400 \mu\text{m}$ ), including all the painted layers, from the ground layer to the varnish. To prepare the cross sections, the samples are embedded in polyester resin polymerised by a peroxo organic catalyser, before cutting with a diamond saw and eventual polishing with diamond paste (6  $\mu\text{m}$  and 2  $\mu\text{m}$ ).

## 3 Results

### 3.1 ESRF-ID31 XRD high resolution

Analysis achieved at the ID31 beamline permitted obtaining of global averaged diffraction diagrams with minor instrumental broadening and with high angular resolution on painting cross sections MGN10 and MGN12. Thus, after Rietveld refinement, it is possible to obtain quantitative analysis in spite of a large contribution to the signal diffraction of the resin embedding the sample: this amorphous matter induces a high background in the diagram, characterised by a broad peak at about  $5.5^\circ$  ( $2\theta$ ) or 0.45 nm ( $d$ ) (Fig. 2). However, it is not possible by this way to take into account of the stratigraphy in the cross section and simultaneously to obtain single X-ray diffraction diagrams

Sample	Position on the panel	Panel	Masterpiece	Museum
MGN1	section 13035-B23	The Resurrection	Isenheim altarpiece	Museum of Unterlinden, Colmar
MGN3	section 13036-H22	The Resurrection	Isenheim altarpiece	Museum of Unterlinden, Colmar
MGN7	section 13037-N26	The Visit of Saint Anthony to Saint Paul the Hermit	Isenheim altarpiece	Museum of Unterlinden, Colmar
MGN8	section 13038-P10	The Concert of Angels	Isenheim altarpiece	Museum of Unterlinden, Colmar
MGN10	section 13039-A12	The Concert of Angels	Isenheim altarpiece	Museum of Unterlinden, Colmar
MGN12	section 13040-K13	The Concert of Angels	Isenheim altarpiece	Museum of Unterlinden, Colmar
G1	section 13875		The Crucifixion	Kunstmuseum, Basel
G4	section 13877		The Crucifixion	Kunstmuseum, Basel

TABLE 1 List of the paint samples analysed

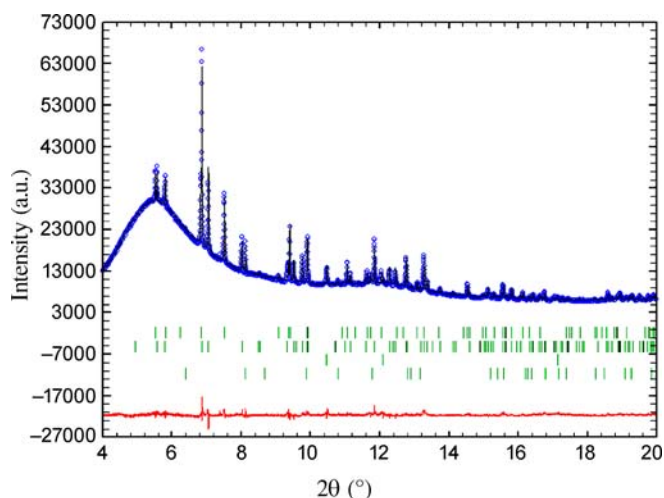


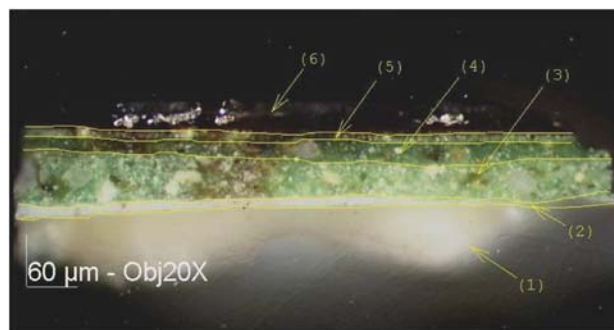
**FIGURE 2** Rietveld plot of MGN10 obtained with FULLPROF [8] ( $R_{wp} = 18.0$ ,  $\chi^2 = 2.05$ ). Observed (dots) and calculated (solid line) synchrotron powder diffraction patterns are shown together with the difference curve below. The vertical ticks indicate the reflection positions for the three phases: (1) hydrocerussite; (2) cerussite; (3) gold; (4) calcite

corresponding to the respective specific layers. This is not a problem in the MGN10 case where the sample consists of a unique 40  $\mu\text{m}$ -thick white layer beneath a thin gold foil. Interpretation of the data from MGN12 is more com-

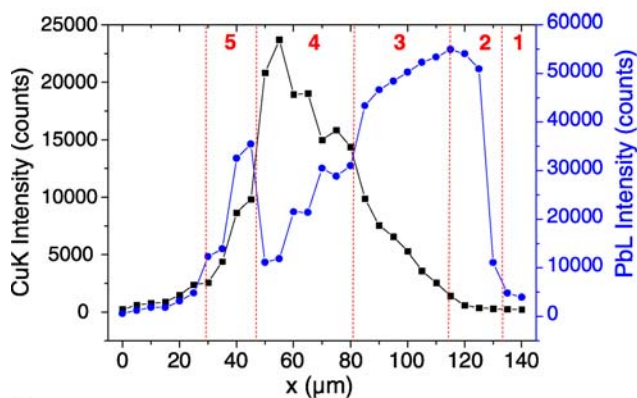
plex because of the great heterogeneity of the sample, the stratigraphy of which includes a white priming layer and two coloured layers (mixtures of blue, green, red and white pigments).

Previous determination of the structure of the hydrocerussite achieved by P. Martinetto et al. [17] made possible quantitative analysis of the lead carbonates. The quality of the diagrams (high counting statistics and angular resolution) leads to data modelling with higher sensitivity and accuracy. An example of Rietveld refinement of MGN10 is shown in Fig. 2. The results show that the paint sample is composed of two lead carbonates, gold and calcite with the following respective mass fractions: hydrocerussite 24.6% ( $\pm 0.6$ ), cerussite 49.9% ( $\pm 1.0$ ), gold 2.8% ( $\pm 0.3$ ), calcite 22.7% ( $\pm 1.1$ ). The deviations of the refined parameters were scaled with the Berar factor [18]. Therefore, the lead white is composed of two lead carbonates in the proportion of 33% for hydrocerussite and 67% for cerussite. The amount of calcite is relatively important and could be due to the presence of a ground layer in the sample. The use of this matter mixed with animal glue is well known during this period [4].

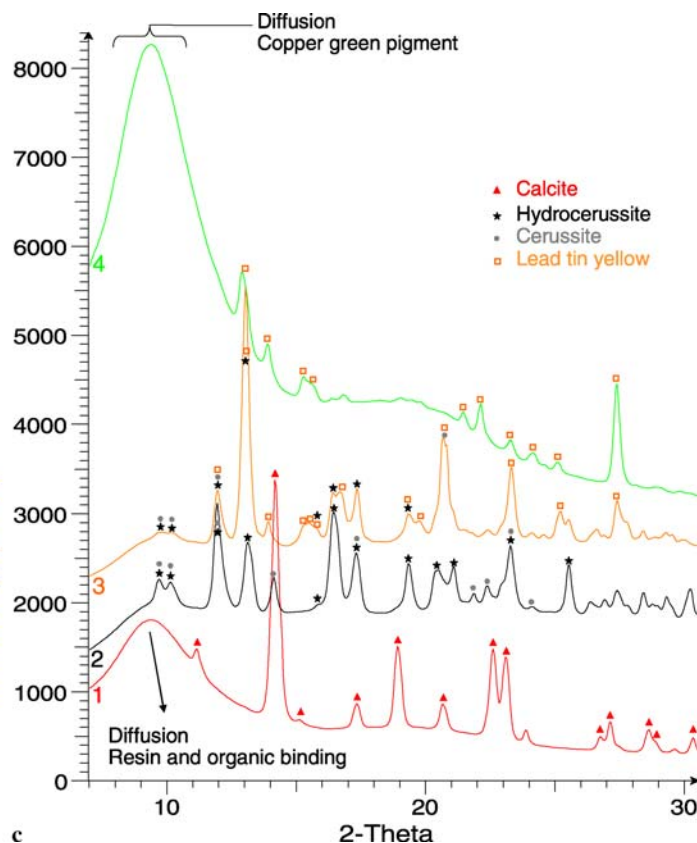
In MGN12, the exact global composition obtained is: hydrocerussite: 13.4% ( $\pm 1.3$ ); cerussite: 15.3% ( $\pm 1.4$ ); azurite ( $2\text{CuCO}_3 \cdot \text{Cu}(\text{OH})_2$ ): 68.9% ( $\pm 5.1$ ); quartz: 2.4% ( $\pm 1.7$ ). The proportions of lead minerals are: hydrocerussite 47%, cerussite 53%.



**a**



**b**



**c**

**FIGURE 3** Analysis by SR-micro XRD and XRF of MGN7. (a) Optical microscope observation of the MGN7 cross section embedded in resin, magnification:  $\times 20$ . (b) Analysis by XRF on a line through the stratigraphy of the cross section, from the outer to the inner layer. The intensities of the Cu K and the Pb L rays are plotted as a function of the analysed points. On this graph, some virtual limits of the different layers have been represented. (c) SR- $\mu$ XRD patterns corresponding to four points selected in the different layers 1, 2, 3 and 4. These data have been collected simultaneously with the XRF. Layer 1: calcium carbonate preparation layer; layer 2: priming layer made of lead carbonates (hydrocerussite and cerussite); layers 3, 4, 5: green copper pigments in mixture with lead tin yellow and lead carbonates; layer 6: organic layer, varnish

### 3.2 Analysis by SR-micro X-ray diffraction in the reflection mode

Analysis by  $\mu$ XRD permits obtaining of a better characterisation of the pigment mixtures, layer by layer in the paint stratigraphy. However, the quantification and the detection of minor phases are possible only when the pigments are well crystallised:  $\mu$ -XRD is not appropriate for the identification of amorphous coloured hybrid materials, such as copper resinates, copper acetates, lakes, etc.

An example is given by the study of the cross section MGN7 (Fig. 3a). The observations by SEM/EDS of the sample have permitted localising of the main elements constituting the pigments. The first layer of this sample, the so called ground layer, is composed of calcium carbonate. Then, the priming layer is constituted of lead white, and is followed by three copper-based green layers including the lead tin yellow pigment, and finally by a thin layer of varnish.

Figure 3c shows examples of diagrams on characteristic points of analysis in the different layers. Only four main compounds were identified: calcite in the preparation (layer 1), lead tin yellow  $2\text{PbO}\cdot\text{SnO}_2$ , hydrocerussite and a small amount of cerussite in the pigment layers 2 to 5. This means that green-copper pigments are amorphous. This is corroborated by the observation of an intense diffuse signal when a large amount of copper is detected by  $\mu$ XRF in layer 4 (Fig. 3b). The different proportions of the amorphous pigment induce the signal variation through the layers. Concerning the diffuse information, the broad peak at low angles in the preparation layer diagram, corresponds to the diffusion of X-rays by the resin and/or the organic binding.

If focused on the lead white pigment, our analytical goal is to quantify the hydrocerussite to cerussite ratio of the lead white pigments. In this case, on MGN7, it is possible that the priming layer is composed only by lead carbonates: all lines on the diffraction image are attributed to the lead white. Good fit parameters have been obtained in the Rietveld refinement analysis as well as an approximate proportion of the two minerals. The hydrocerussite is the main component; cerussite contributes about twenty five percent to the global composition (hydrocerussite: 75% ( $\pm 6$ ); cerussite: 25% ( $\pm 7$ ); Rp: 14.6; Rwp: 13.1; Rexp: 17.44;  $\chi^2$ : 0.561).

Often in some pigment layers of the cross sections, difficulties have been encountered in quantifying this ratio with the use of a microbeam of only  $6\ \mu\text{m}^2$ , due to the following reasons:

- A microbeam does not permit to analyse of a large quantity of grains, and probes a grain distribution which may be very different from a statistical distribution in all crystallographic orientations. This point is required in the powder diffraction theory for accuracy of the quantitative analysis. In Fig. 4, only two grains of cerussite are observed among several tens of grains of hydrocerussite. This may induce erroneous quantification results. Then, it is always necessary to compare the one-dimensional data with the images of diffraction rings. So, we can verify and establish the validity of the quantitative results.
- Some additional difficulties may occur because of the dominating contribution of one pigment in the diffracted signal. This is the case for the lead tin yellow pigment:

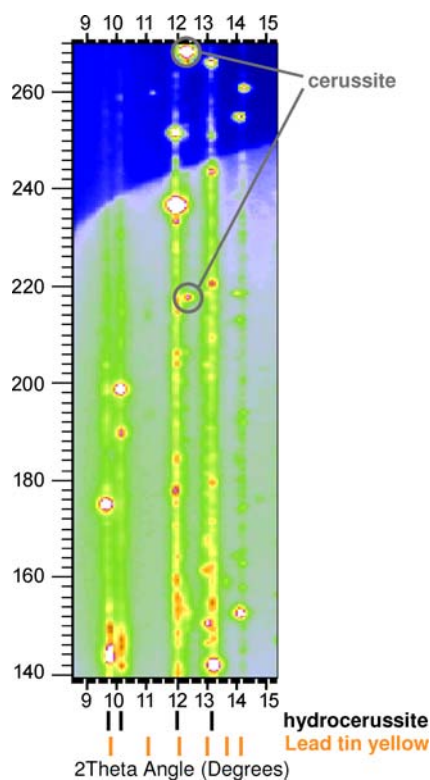


FIGURE 4 XRD 2D image observation with Fit2D ESRF package of a point analysis in the priming layer in the painting cross section of MGN7 (beam size =  $3.8 \times 1.4\ \mu\text{m}^2$  (H $\times$ V),  $E = 16\ \text{keV}$ ). Two grains of cerussite (circled reflections) in hydrocerussite matrix are observed on the unrolled diffraction rings. All the lines are the contribution of the diffracted signal of the hydrocerussite phase

large grains (about 10 to 20  $\mu\text{m}$ ) made of nanocrystals of  $2\text{PbO}\cdot\text{SnO}_2$  contribute more than eighty percent to the total diffracted signal on some points of the analysis.

The lead white priming layer of the MGN8 cross section is mainly constituted by hydrocerussite. The determination of the ratio (hydrocerussite/cerussite) is not possible because of the size of the grains: large and very intense spots are observed on the diffraction images and induce irregularities in the patterns. Consequently, it seems that we have two varieties of lead white with different grinding treatments and different ratios between the two lead carbonates.

### 3.3 Analysis by SR-micro X-ray diffraction in transmission mode

Problems with statistical data encountered for the phase quantification have required additional analysis at the ESRF-ID22 beamline in transmission mode, directly on a small sample fixed on a glass capillary. The method is attractive because no sample preparation is needed and the whole sample can be analysed. The use of this geometry allows obtaining of a signal projection of the object in two dimensions and then to obtain a map of the crystalline composition in the case of painting layers oriented parallel to the beam axis.

Analysis by  $\mu$ XRF- $\mu$ XRD of a “soldiers armour” sample (MGN3) show that two different layers exist: a 25  $\mu\text{m}$  thick priming layer constituted of lead white pigment and a sec-

ond layer composed of lead white associated with stibnite, and antimony sulphide  $\text{Sb}_2\text{S}_3$  that gives the grey metallic colour. The use of stibnite was not common during this period in Germany [19, 20]. Here the striking result is the observation of the stibnite distribution inside the lead white layer thanks to a  $\mu$ -XRD map and the quantification of the lead carbonates in each layer.

Figure 5a shows the integrated X-ray diffraction pattern, i.e. the sum of the diffraction signals from all the points of analysis. Several regions of interest in the  $2\theta$  angle are

defined around individual strong reflections of stibnite and hydrocerussite with the Artemis software [21]. After calculation of the net peak area for each region of interest in  $2\theta$ , the corresponding maps are obtained (Fig. 5b). The first on the left, corresponds to the hydrocerussite (reflection  $\langle 015 \rangle$  for a region of interest centered on  $12.06^\circ$  in  $2\theta$  angle). The second and the third correspond to the stibnite phase for different reflections  $\langle 202 \rangle$  and  $\langle 302 \rangle$  respectively at around  $9.93^\circ$  ( $2\theta$ ) and at around  $12.65^\circ$  ( $2\theta$ ). The corresponding maps permit distinguishing of the two dis-

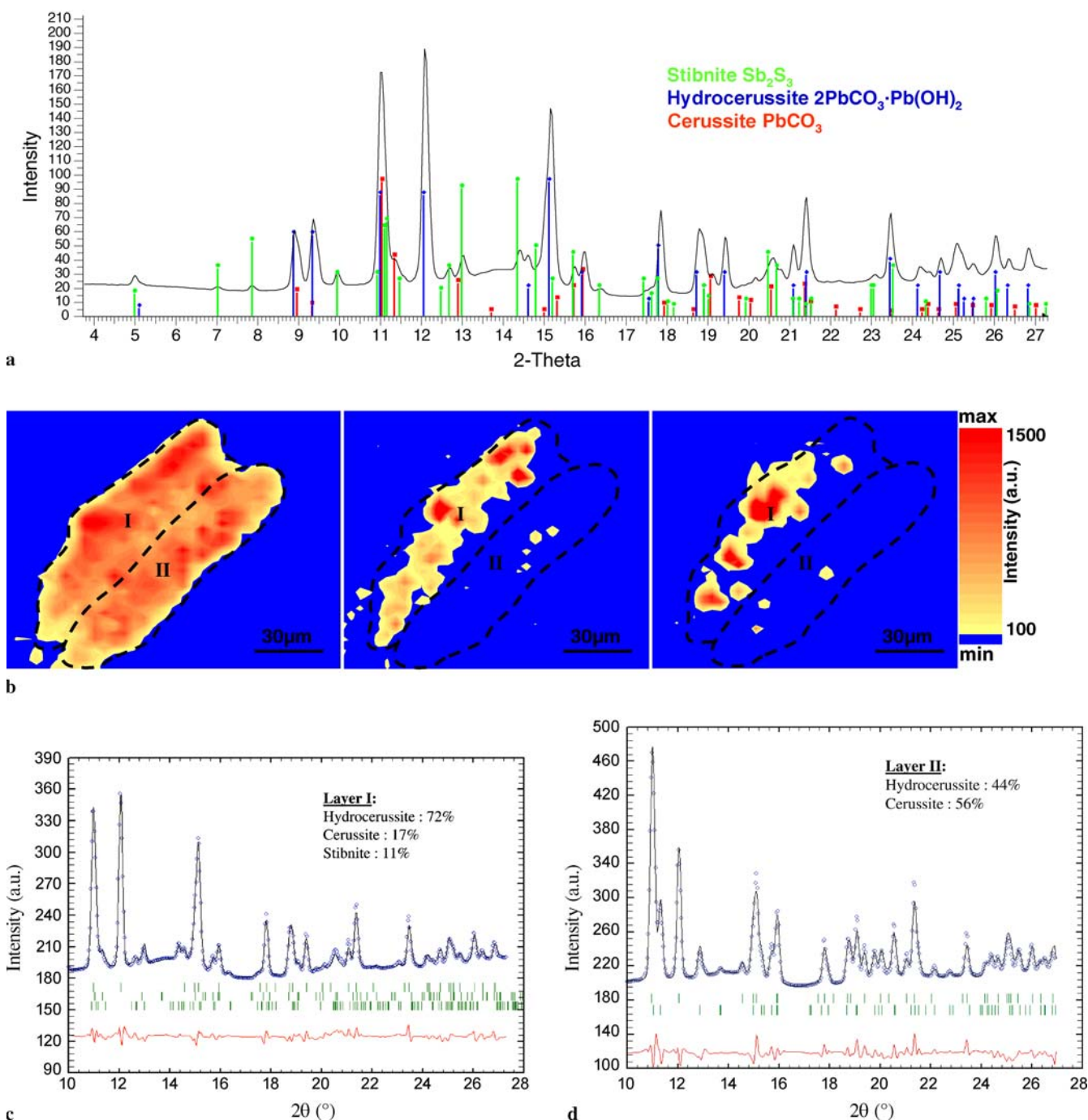


**FIGURE 5** Study by SR- $\mu$ XRD in transmission mode of the sample MGN3. (a) Pattern corresponding to the transmission diffraction signal of the whole sample (software EVA). (b) Maps of different mineral phases. From left to right: hydrocerussite  $\langle 015 \rangle$ , stibnite  $\langle 202 \rangle$ , stibnite  $\langle 302 \rangle$ . (c, d) Rietveld plots of the layers I and II of MGN3 obtained with FULLPROF. Quantitative results on the layer I and II are given as mass fraction

tinct layers: I and II. The stibnite phase is mainly present in layer I in the form of grains. Some artifacts appear in layer II, maybe due to some punctual saturation of the detector and to the contribution of another phase in the selected region of interest. Moreover, in order to avoid the visualisation of two different phases simultaneously on the same map because of the overlapping of peaks, we have had to select individual diffraction peaks of weak intensity for the stibnite.

Average patterns corresponding to the specific layers I and II have been plotted (Fig. 5c and d). So, we obtain patterns with better statistics that permit a correct Rietveld refinement analysis for quantitative information. The amount of stibnite is relatively low, about 11% in layer I, an amount sufficient to give the desired grey metallic shade and we can verify that selection of the limit of the two layers is correct because layer II does not contain any stibnite. Two different compositions of the lead white pigment are found: (hydrocerussite/cerussite) 81%/19% and 44%/56% respectively for layer I and layer II. This difference can not result from the phase degradation with time because of the high stability of these minerals and the protective action of the varnish and the binder, which prevent the transformation of one phase into the second one caused by the diffusion of the water and carbon dioxide needed for this.

Same results have been observed for the sample MGN12. The SR-transmission X-ray diffraction analysis at ID22 allowed us to determine different ratios (hydrocerussite to cerussite) in the copper layers and in the priming layer whereas the X-ray high resolution diffraction at the beamline ID31 gave global results.

That means Grünwald has intentionally used two different white lead pigments to compose this part of his masterpiece.

#### 4 Discussion

All these methods using synchrotron radiation X-ray diffraction supply important information about the nature of pigments. The use of a large beam with high angle resolution provides an accurate mean for quantitative analysis but also brings some non-discriminated information on the composition. The complex microstructure of the layers and the large variety of the pigments are overlooked by this method. The use of a microbeam opens the way to spatially-resolved and layer-selective analysis. However it can cause some sampling problems if not enough grains contribute to the signal, or if the granulometry is too coarse. That may bring some errors in the quantitative analysis (estimated at around 15%). However, we were able to distinguish between four main composition groups of lead white (Table 2). A corresponds to a hydrocerussite pigment (cerussite < 5%), B to a mixture mainly constituted by hydrocerussite (cerussite  $\approx$  20%), C to a mixture of both lead carbonates in a similar proportion, and D to a cerussite pigment (cerussite > 95%).

A test of the validity of two approaches (with high resolution, which provides accurate quantitative information, and in transmission mode) has consisted of comparing the global results for the MGN12 sample. Similar global hydrocerussite to cerussite ratios have been obtained according to the eval-

uated errors for the microbeam analysis, (47%/53% for the high resolution mode and 55%/45% in transmission mode).

Reflection SR- $\mu$ -XRD brings good results regarding the possible analysis of each specific layer even if it is difficult to evaluate the attenuation length of X-rays in the sample: for a beam footprint localised on a specific layer, some grains located deeper belonging to another layer might also contribute to the diffraction signal. Moreover, the diffraction signal can not be exploited at a low angle because of its re-absorption through the resin and the sample itself (shadowing effects are noticeable on the 2D diffraction image in Fig. 1a). The high contribution of the diffuse signal due to the resin is also a problem.

Use of  $\mu$ XRD in transmission mode turns out to be a particularly well suited technique for many reasons:

1. No sample preparation is needed.
2. The high spatial resolution allows mapping of the different phases in each painting layer. However, sometimes it is difficult to put the paint layers plane in the axis of the beam in order to get results that are easy to interpret.
3. A reasonable average of diffraction diagrams in a selected layer allows obtaining of quantitative analysis, although the beam size is similar to the grain size.
4. As there is no embedding resin, the signal to noise ratio is increased and allows in addition, accurate quantification as well as detection of minor phases. Moreover, it is possible to observe amorphous phases (pigments, binders, varnishes) that contribute to the pattern as a diffuse signal at a low angle. The intensity of the broad peaks is directly correlated to the amount of amorphous matter.
5. Re-absorption of the signal by the sample itself is less important (than in the other approaches) if the X-ray energy is higher and the 2D diffraction images are less noisy.

A comparison of the quantitative results on the different samples has been achieved. Different ratios were obtained (Table 2). At present, we are studying other samples from Grünwald and from contemporary painters. The present work shows that various lead white compositions have been used and that the variability in composition and granularity is linked to the different sources available. This conclusion is supported by the mention of three different white pigments on the Frankfurt Market at the beginning of the XVIth century [6] from Venetia, Antwerp, with the last being of unknown origin. The manufacturers in Venetia and Antwerp were very famous, so the common lead white could correspond to an ordinary and cheaper pigment from elsewhere.

The choice of a specific pigment, in a particular case, demonstrates the know-how of the artist. The choice can be influenced by the function of the pigment, e.g. to whiten a layer or to realize the priming layer or/and for economical reasons. Indeed, it seems that the priming layers are most often composed by a mixture of hydrocerussite and cerussite (groups B or C) and on the contrary the pigment layers are composed of hydrocerussite in majority (groups A or B). The sample MGN3 very well illustrates this assumption because two types of pigments have been clearly identified for these different uses.

If we focus our attention on the priming layer, we could consider that the artist has made only one application of the

		Samples							
		The Resurrection Isenheim		The Visit of St Anthony Isenheim	The Concert of Angels Isenheim			The Crucifixion Basel	
		MGN1	MGN3	MGN7	MGN8	MGN10	MGN12	G1	G4
Paint Layer	Priming (thickness)	A	C (20 μm)	B (5 μm)	B (5 μm)	D	C (15 μm)	B (11 μm)	
	Grey Pigment (Sb <sub>2</sub> S <sub>3</sub> )		B						A
	Green pigment (Cu)			A	A		B	A	
	White pigment with gold foil					C			

**TABLE 2** Lead carbonates composition of the different paint samples analysed by SR-XRD. Group A: (hydrocerussite > 95%); group B: (hydrocerussite ≈ 80%); group C: (hydrocerussite = cerussite); group D: (cerussite > 70%)

pigment on the whole surface of a specific panel. Moreover, we can note that it is probably not the case on considering the composition (ratio of the lead carbonates, and the presence of other mineral compounds like calcite or quartz) and the thickness of the priming layers, which have been reported in Table 2.

## 5 Conclusions

Several approaches have been tested by SR-XRD for the study of painting samples from Grünewald's masterpieces and we have shown how qualitative and quantitative interpretations of the XRD images give relevant information on the pigments and can help us to understand the painters technique. In particular, the mapping mode in  $\mu$ -XRD has permitted identification and localising of the different mineral phases in the stratigraphy, and above all the obtaining of average diffraction diagrams corresponding to a specific layer for a quantitative analysis of lead whites.

Obviously, in some cases, the use of complementary techniques like XRF and XANES can help us to solve uncertainties when analysing other pigments like copper greens.

Results obtained by X-ray diffraction revealed that the ratio of the two lead carbonate phases can be very different depending on the sample and could be characteristic of a period, the know-how, and the geographical origin. Moreover, these data could permit relating of the composition of painting samples with ancient recipes, i.e. with the chemical conditions of synthesis and preparation of lead carbonates.

This highlights another aspect: the notion of the "paint pot" used for a given period in a workshop being characterized by a physico-chemical signature (composition, grain size). It is necessarily related to relevant practices and chemical expertise. Complexity and dissimilarities in composition can be linked to several sources of raw material or different preparation processes.

**ACKNOWLEDGEMENTS** This research has been ongoing since 2004 as part of a long term project at the ESRF (experiment CH1777).

The authorization and access to samples was granted in the framework of a recent research programme at the C2RMF dedicated to the masterworks of Grünewald. We wish to thank Eric Laval, Sandrine Pagès, Anna Principaud of the C2RMF and curators for their participation to the general study of the palette of Grünewald, and also Jean Susini, M. Cotte, F. Fauth and A. Fitch at the ESRF, Grenoble.

## REFERENCES

- 1 E. Welcomme, P. Walter, E. van Elslande, G. Tsoucaris, *Appl. Phys. A* **83**, 551 (2006)
- 2 H. Le Bonniec, *Pline l'Ancien, Histoire naturelle, XXXIV* (Les Belles Lettres, Paris, 1983)
- 3 J.M. Croisille, *Pline l'Ancien, Histoire naturelle, XXXV* (Les Belles Lettres, Paris, 1985)
- 4 R. Billinge, L. Campbell, J. Dunkerton, S. Foister, J. Kirby, J. Pilc, A. Roy, M. Spring, R. White, *Nat. Gallery Tech. Bull.* **18**, 6 (1997)
- 5 M. Cotte, E. Checroun, J. Susini, P. Walter, *Appl. Phys. A* (this volume) (2007)
- 6 R. Riepertinger (Ed.), *Das Rätsel Grünewald*, Catalog of "Bayerische Landesausstellung, Aschaffenburg 2002/2003", Augsburg (2002)
- 7 A.N. Fitch, *J. Res. Nat. Inst. Stand. Technol.* **109**, 133 (2004)
- 8 J. Rodriguez-Carjaval, *Abst. Satellite Meeting on Powder diffraction of the XVth IUCR Congress* (1990), p. 127
- 9 H.M. Rietveld, *J. Appl. Phys.* **2**, 65 (1969)
- 10 J.I. Langford, D. Louër, *Rep. Prog. Phys.* **59**, 131 (1996)
- 11 A. Somogyi, R. Tucoulou, G. Martinez-Criado, A. Homs, J. Cauzid, P. Bleuet, S. Bohic, A. Simionovici, *J. Synchrotron. Radiat.* **12**, 208 (2005)
- 12 A. Somogyi, M. Drakopoulos, L. Vincze, B. Vekemans, C. Camerani, K. Janssens, A. Snigirev, F. Adams, *X-ray Spectrom.* **30**, 242 (2001)
- 13 A.P. Hammersley, *Synch. Radiat. News* **2**, 24 (1989)
- 14 N. Salvado, T. Pradell, E. Pantos, M.Z. Papiz, J. Molera, M. Seco, M. Vendrell-Saz, *J. Synchrotron. Radiat.* **9**, 215 (2002)
- 15 J.C. Labiche, J. Segura-Puchades, D. Van Brussel, J.P. Moy, *ESRF Newslett.* **25**, 41 (1996)
- 16 M. Menu, J.-J. Ezrati, E. Laval, S. Pagès, A. Principaud, J.-P. Rioux, P. Walter, E. Welcomme, W. Nowik, *La technique de Grünewald et de ses contemporains*, éd C2RMF, Musée de Colmar, Eu-Artech (2007)
- 17 P. Martinetto, M. Anne, E. Dooryhée, P. Walter, G. Tsoucaris, *Acta Cryst. C* **58**, i82 (2002)
- 18 J.F. Bézar, P. Lélann, *J. Appl. Cryst.* **24**, 1 (1991)
- 19 M. Ferretti, G. Guidi, P. Moiola, R. Scafe, C. Seccaroni, *Stud. Conserv.* **36**, 235 (1991)
- 20 M. Spring, R. Grout, R. White, *Nat. Gallery Tech. Bull.* **24**, 96 (2003)
- 21 G. Gros, N. Pascal, S. Pelletier, ARTEMIS-Software for generating elemental maps using X-ray fluorescence spectra, European Synchrotron Radiation Facility (2001)